Single beam mapping of nonlinear phase shift profiles in planar waveguides with an embedded mirror

Yoav Linzon,[1*] Yaron Shavit,[1] Moshe Elazar,[1] Roberto Morandotti,[2] Maite Volatier-Ravat,[3] Vincent Aimez,[3] Richard Ares,[3] and Shimshon Bar-Ad[1]

[1] *School of Physics and Astronomy, Raymond and Beverly Sackler Faculty of Exact Sciences, Tel-Aviv University, Tel Aviv 69978, Israel*

[2] *Universite' du Quebec, Institute National de la Recherche Scientifique, Varennes, Quebec J3X 1S2, Canada*

[3] *Centre de Recherche en Nanofabrication et en Nanocaracterisation, Universite de Sherbrooke, 2500 Boulevard Universite, Sherbrooke, J1K2R1, Canada*

** E-mail: linzonyo@post.tau.ac.il*

Abstract: We demonstrate a technique for a single shot mapping of nonlinear phase shift profiles in spatial solitons that are formed during short pulse propagation through one-dimensional slab AlGaAs waveguides, in the presence of a focusing Kerr nonlinearity. The technique uses a single beam and relies on the introduction of a lithographically etched reflective planar mirror surface positioned in proximity to the beam's input position. Using this setup we demonstrate nonlinearity-induced sharp lateral phase variations for certain initial conditions, and creation of higher spatial harmonics when the beam is in close proximity to the mirror.

© 2007 Optical Society of America

OCIS codes: (130.2790) Guided waves; (190.0190) Nonlinear optics; (190.5530) Pulse propagation and solitons; (230.4000) Microstructure fabrication; (230.7390) Waveguides, planar.

References and links

1. See, for example: T. Dauxois and M. Peyrard, *Physics of Solitons* (Cambridge University Press, London, 2006).
2. See, for example: J. R. Taylor, *Optical Solitons - Theory and Experiment* (Cambridge University Press, New York, 1999).
3. See, for example: S. Trillo and W. E. Torruellas, *Spatial Solitons* (Springer-Verlag, Berlin, 2001).
4. O. Jedrkiewicz, J. Trull, G. Valiulis, A. Piskarskas, C. Conti, S. Trillo, and P. Di Trapani, "Nonlinear X waves in second-harmonic generation: Experimental results," Phys. Rev. E **68,** 026610 (2003).
5. P. Di Trapani, G. Valiulis, A. Piskarskas, O. Jedrkiewicz, J. Trull, C. Conti, and S. Trillo, "Spontaneously generated X-shaped light bullets," Phys. Rev. Lett. **91,** 093904 (2003).
6. J. Meier, G. I. Stegeman, D. N. Christodoulides, Y. Silberberg, R. Morandotti, H. Yang, G. Salamo, M. Sorel, and J. S. Aitchison, "Beam interactions with a blocker soliton in one-dimensional arrays," Opt. Lett. **30,** 1027–1029 (2005).
7. R. Jin, C. L. Chuang, H. M. Gibbs, S. W. Koch, J. N. Polky, and G. A. Pubanz, "Picosecond all-optical switching in single-mode GaAs/AlGaAs strip-loaded nonlinear directional couplers," Appl. Phys. Lett. **53,** 1792–1793 (1988).
8. H. S. Eisenberg, Y. Silberberg, R. Morandotti, A. R. Boyd, and J. S. Aitchison, "Discrete spatial optical solitons in waveguide arrays," Phys. Rev. Lett. **81,** 3383–3386 (1988).
9. J. Meier, J. Hudock, D. Christodoulides, G. Stegeman, Y. Silberberg, R. Morandotti, J. S. Aitchison, "Discrete Vector Solitons in Kerr Nonlinear Waveguide Arrays," Phys. Rev. Lett. **91,** 143907 (2003).

#84738 - $15.00 USD Received 2 Jul 2007; revised 30 Aug 2007; accepted 2 Sep 2007; published 6 Sep 2007

10. See, for example: J. D. Jackson, *Classical Electrodynamics*, 3rd edition (John Wiley and Sons, New York, 1998), pp. 352-366, 378-389.
11. The BPM code is available for free at http://www.freeBPM.com.
12. H. S. Eisenberg, R. Morandotti, Y. Silberberg, S. Bar-Ad, D. Ross, and J. S. Aitchison, "Kerr spatiotemporal self-focusing in a planar glass waveguide," Phys. Rev. Lett. **87,** 043902 (2001).
13. Y. Linzon, I. Ilsar, D. Cheskis, R. Morandotti, J. S. Aitchison, and S. Bar-Ad, "Near-field imaging of nonlinear pulse propagation in planar silica waveguides," Phys. Rev. E **72,** 066607 (2005).
14. J. P. Gordon, "Theory of the soliton self-frequency shift," Opt. Lett. **11,** 662–664 (1986).
15. J. A. Giordmaine, "Mixing of light beams in crystals," Phys. Rev. Lett. **8,** 19–20 (1962).
16. G. Bartal, O. Manela, and M. Segev, "Spatial four wave mixing in nonlinear periodic structures," Phys. Rev. Lett. **97,** 073906 (2006).
17. D. V. Skryabin and A. V. Yulin, "Theory of generation of new frequencies by mixing of solitons and dispersive waves in optical fibers," Phys. Rev. E **72,** 016619 (2005).
18. A. Efimov, A. V. Yulin, D. V. Skryabin, J. C. Knight, N. Joly, F. G. Omenetto, A. J. Taylor, and P. Russell, "Interaction of an Optical Soliton with a Dispersive Wave," Phys. Rev. Lett. **95,** 213902 (2005).
19. S. Flach, V. Fleurov, A. V. Gorbach, and A. E. Miroshnichenko, "Resonant Light Scattering by Optical Solitons," Phys. Rev. Lett. **95,** 023901 (2005).
20. D. Mandelik, Y. Lahini, and Y. Silberberg, "Nonlinearly Induced Relaxation to the Ground State in a Two-Level System," Phys. Rev. Lett. **95,** 073902 (2005).
21. A. Avidan, Y. Lahini, D. Mandelik, and Y. Silberberg, "Ground-state selection as a four-wave-mixing process," Phys. Rev. A **73,** 063811 (2006).

---

1. Introduction, theoretical and numerical background

1.1. Introduction

Solitons are self-regulating nonlinear excitations, with fascinating properties that are intermediate between waves and particles [1]. Nonlinear optics provide the most common and elementary manifestation of solitons [2], including spatial solitons [3]. Among the most important quantities that characterize a nonlinear excitation are the phase profile that is accumulated during its propagation, and the phase shift with respect to its linear counterpart. Traditionally, these quantities are measured using rather complex two-beam techniques [4, 5, 6]. In this paper we demonstrate a simple, single beam technique for measuring the phase shift profile of spatial solitons in 2D slab waveguides. Our method relies on the introduction of an embedded planar mirror inside the waveguide, the excitation of a soliton in close proximity to this mirror and the interference formed by the soliton and the wave reflected from the mirror. The paper is organized as follows: in Sec. 1 we briefly discuss the theoretical background of solitons and their nonlinear phase evolution. In Sec. 2 the optical experiment is described, the geometry of the sample is introduced, and our sample is compared to a sample with shallow-etched barrier interfaces, of the type that is traditionally used, *i.e.* in the study of the interaction of spatial solitons with micro-structured inhomogeneities [7, 8, 9]. In Sec. 3 our experimental results are shown, including the measurement of the nonlinear phase shift profile of a spatial soliton, the observation of nonlinearity-induced sharp lateral phase variations, and the creation of higher spatial harmonics when the soliton is launched near the mirror, due to proximity effects. In Sec. 4 we summarize our main results and conclusions.

1.2. Theoretical and numerical background

While the intensity properties of spatial solitons in slab waveguides have been studied extensively [3], it is interesting to note that several phase-related properties of these solitons are usually assumed without their explicit measurement. Writing the electric field associated with an initial excitation as $E(x,z) = |E(x,z)|e^{i\phi(x,z)}$, with x being the lateral waveguide direction and z being the propagation direction (assuming confinement in the y direction), $\phi(x,z)$ is the phase accumulation and $\beta(x,Z) = \frac{\partial\phi}{\partial z}|_{z=Z}$ is the propagation constant. While a linear wave that traverses the waveguide has a propagation constant that falls in the allowed region of the

#84738 - $15.00 USD Received 2 Jul 2007; revised 30 Aug 2007; accepted 2 Sep 2007; published 6 Sep 2007
(C) 2007 OSA

geometrical waveguide dispersion [10], a nonlinear soliton has a higher propagation constant, corresponding to a bound state penetrating into the semi-infinite gap where no linear guided modes exist; indeed, this is the key property that enables the non-dispersive nature of these nonlinear excitations, *i.e.* a spatial localization occurring at higher optical intensities. Assuming the slowly varying envelope approximation, the paraxial approximation, and energy conservation for the forward traveling wave, the 2D electromagnetic field dynamics in a slab Kerr waveguide can be described by the well known nonlinear Schrödinger equation (NLSE) [1−3]. The solution of the NLSE of the form $E(x,z) \sim E(x)e^{i\beta z}$ leads to an eigenvalue equation $i\frac{\partial E}{\partial z} \sim -\beta E$, where β is in the gap.

To illustrate the importance of ϕ and β in spatial soliton formation, Figs. 1 and 2 show solutions of the NLSE obtained from beam propagation method (BPM) simulations [11].

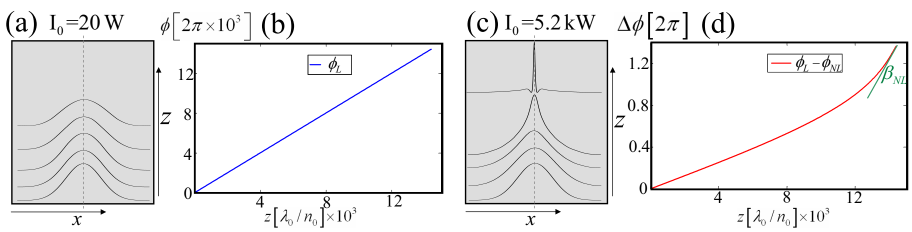

Fig. 1. **(a), (b)** Low power (20 W) and **(c), (d)** high power (5.2 kW) simulations of Eq. (1) at $\lambda_0 = 1.5\ \mu m$ for a 100 μm-wide input Gaussian wave packet, with flat phase-front initial conditions, over a propagation length of z=6.5 mm in a planar AlGaAs waveguide. **(a), (c)**: Intensity evolution ($|E(x,z)|^2$). **(b)** Phase evolution $\phi(z)$ (estimated at a central x position indicated by the dashed lines in (a),(c)). **(d)** Phase difference $\Delta\phi(z)$ between the nonlinear propagation (c) and the linear propagation (a),(b), at the same x position.

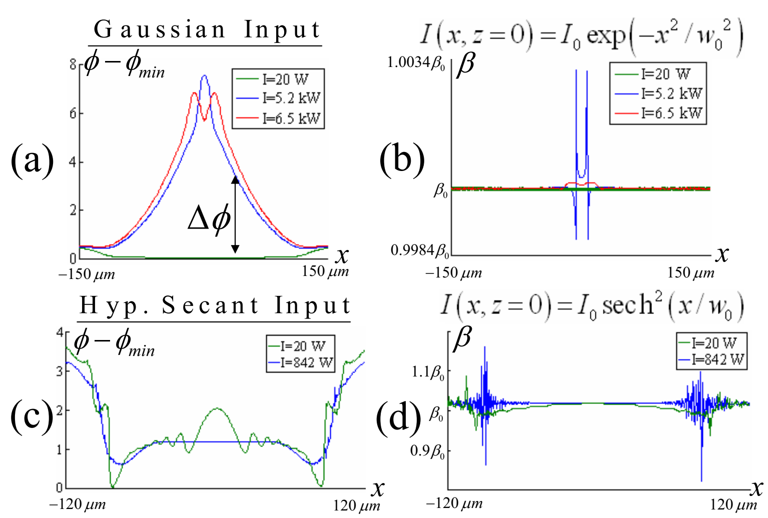

Fig. 2. Simulated phase profiles (left panels, **(a)** and **(c)**) and propagation constant profiles (right panels, **(b)** and **(d)**) at the output following linear (green lines) and nonlinear (blue/red lines) propagation over a 6.5 mm-long 2D AlGaAs waveguide. The input beam intensity profile is Gaussian with a width of 100 μm in the top panels (**(a)** and **(b)**), while it has the form a square Hyperbolic Secant with a width of 13 μm in the bottom panels (**(c)** and **(d)**). In all cases, the excitation wavelength is $\lambda_0 = 1.5\ \mu m$.

#84738 - \$15.00 USD Received 2 Jul 2007; revised 30 Aug 2007; accepted 2 Sep 2007; published 6 Sep 2007
(C) 2007 OSA

It is well known that a low-power beam slowly diffracts when propagating along the z direction (Fig. 1(a)). The accumulated phase at the center of the beam (Fig. 1(b)) is linear with a slope of approximately unity in the dimensionless units of Fig. 1(b). Note that the slope $\beta_0 = \frac{\Delta\phi}{\Delta z} \approx 2\pi/\lambda_0$ is approximately the plane-wave propagation constant. As the input power is increased, a solitary wave is formed (Fig. 1(c)), and the accumulated phase is different from the case presented in Fig. 1(b). The accumulated phase *difference* relative to Fig. 1(b) is shown in Fig. 1(d), and is indeed nonlinear. The positive slope corresponds to a self-focusing nonlinearity $n_2 > 0$, with a local increase of the propagation constant, associated with its penetration into the semi-infinite gap. Lateral Profiles of the output phases and propagation constants obtained from the above simulations are shown in Figs. 2(a),(b) for different input powers. Beyond a certain threshold power, a spatial breakup occurs that is accompanied by a breakup of the phase profile (Fig. 2(a)) and by the recovery of the linear propagation constant (Fig. 2(b)).

In the well known special case of input beams with the hyperbolic Secant intensity form, while the phase front profile of a low power diffracting beam has a particular pattern (green line in Fig. 2(c)), as a soliton forms it becomes flat and stationary at the beam's center (blue line in Fig. 2(c)). In this case β is uniform and larger than β_0 (Fig. 2(d)).

2. Optical setup and sample composition

2.1. Optical setup

The conventional techniques for measuring nonlinear phase variations are cumbersome, as they require at least *two* beams: the soliton beam of interest, and a reference low-power beam not undergoing the phase change, *i.e.* it linearly diffracts along with the soliton [4, 5, 6]. These methods are illustrated in Figs. 3(a),(b). One realization (Fig. 3(a)) involves coupling the beams at remote locations of the input facet with separate lenses, under similar conditions and with different input powers. When the beams reach the output facet, they have different linear and nonlinear phases. As a result, their overlapping on a nonlinear crystal yields a phase related cross-correlation signal [4, 5]. In another realization the two beams are coupled in close proximity, using the same input lens (Fig. 3(b)). The beams' partial overlap and the resulting coherent interference pattern recorded by an imaging camera contains the required information regarding the soliton's added phase [6]. In both of these techniques the two beams must be coherent and individually stable following their splitting, also implying that the alignment of the sample with respect to both of the input beams is critical.

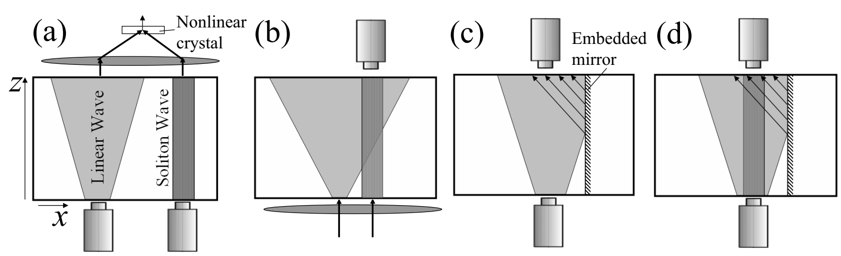

Fig. 3. Possible nonlinear phase shift measurement setups. **(a)** A two-beam setup involving remote coupling with different lenses, following the two beams overlapping on a nonlinear crystal. **(b)** A two-beam setup involving close coupling with the same lens following output facet imaging. (c) and (d): A single beam setup with a plane mirror surface embedded in the waveguide and output facet imaging: **(c)** Low power and **(d)** high power (soliton) beams.

Here we show that by using an embedded mirror surface, oriented parallel to the propagation direction (Figs. 3(c),(d)), a single beam experiment can yield the spatially resolved phase

#84738 - $15.00 USD   Received 2 Jul 2007; revised 30 Aug 2007; accepted 2 Sep 2007; published 6 Sep 2007
(C) 2007 OSA

profile, eliminating any need for multiple beams. In particular, a low-power diffracting beam that is coupled near a mirror (Fig. 3(c)) exhibits interference between its central part and the reflected tails, all having the same wavelength. Even as the power is increased and a spatial soliton is formed, there is some weak background undergoing linear diffraction. Some extent of these diffracting tails then interferes with the soliton (Fig. 3(d)). The output phase difference profile $\Delta\phi(x)$ is then directly measured as it results in phase shifts of the imaging interference pattern. We stress that the interference fringe shift is exactly equal to the nonlinear phase only in the case of *spatial* solitons (which are dispersive in the temporal domain) [2, 3], such as in AlGaAs waveguides. When *spatiotemporal* compression is considered (*i.e.* as self-focusing is observed in both space and time dimensions) [12, 13], it is generally accompanied by a shift of the soliton wavelength [14]. Since this added wavelength shift is unknown without additional measurements, neither of the contributions to the phase change can be extracted from the proposed experimental technique.

2.2. *Sample geometry*

3-layer semiconductor Al_xGaAs_{1-x} waveguides have been used extensively for nonlinear optics applications [7], as well as for studies of soliton propagation in micro-structured waveguide arrays [8, 9]. These samples consist of Clad-Core-Clad sadwiches deposited on top of a GaAs substrate with vertical dimensions designed for single-mode propagation [10] in the near infrared (see Figs. 4(a),(c)). The Aluminum doping levels x=0.18 in the core layer and x=0.24 in the clad layer give rise to a physical vertical refractive index difference of Δn=0.03 at λ_0=1.5 μm, with a core index of n_0=3.34. A 25 μm-wide shallow etching applied to the top clad (Fig. 4(a)) effectively decreases the mode area, and therefore the effective refractive index, of a beam confined to the core [8, 9]. Therefore, shallow etchings serve as local barriers to confined beams.

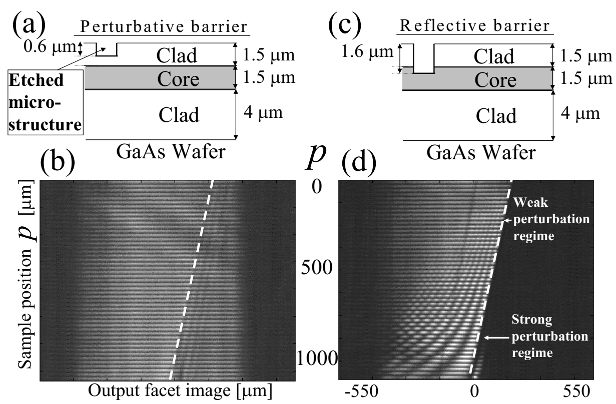

Fig. 4. (a),(c): Vertical sample cross-sections with local barriers formed by **(a)** a shallow 0.6 μm etching, and **(c)** a deep 1.6 μm etching. (b),(d): Output facet images as a function of the sample position p (along the x direction, with respect to the input beam) in samples with a barrier that is **(b)** perturbative (as in (a)) and **(d)** reflective (as in (b)). Both samples have the same length (6.5 mm), and are excited by a low power (100 W) 100 μm-wide Gaussian input beam. The left boundaries of the barriers are indicated by the dashed white lines in (b),(d). The same sample position scale p is used in subsequent figures.

In contrast, a deeply etched interface that penetrates into the core layer (Fig. 4(c)), can inhibit coupled wave transfer from one side of the center to the other, serving as a reflective barrier. The corresponding output facet images, as a function of the input beam position, are shown in Figs. 4(b),(d). Clearly, the diffracting beam crosses almost completely the shallow etched

#84738 - $15.00 USD Received 2 Jul 2007; revised 30 Aug 2007; accepted 2 Sep 2007; published 6 Sep 2007
(C) 2007 OSA

interface, while completely reflecting from the deeply etched interface. In the latter case, the sharp beam cutoff at the barrier interface is evident, as well as the fringe patterns associated with the interference between the original and reflected beams, and the increased degree of overlap between the two beams as the input beam is coupled closer and closer to the barrier. Also note that at input locations that are distant from the center, the fringe spacing changes linearly with the input position, while at locations that are adjacent to the center the fringe spacing changes parabolically. In the former case only the weak diffracting wings are reflected by the mirror (as in Fig. 3(c)), and we therefore refer to this region as the ”weak perturbation regime”. In the latter case, however, both beams are of comparable powers as part of the input beam is already at the interface, and the interference pattern changes nonlinearly with the input position. To this region of excitation we will refer below as the ”strong perturbation regime”.

3. Experimental results

3.1. Phase shift profile mapping

In order to excite spatial solitons in our 6.5 mm-long AlGaAs waveguides, which include an embedded mirror, we use laser pulses of 100 fs duration, 1 kHz repetition rate, and peak powers of up to 5 kW. The input beam is shaped to be elliptical with an height of $\simeq 1.5\ \mu m$ (to enable efficient coupling to the core layer, see Fig. 4(c)) and an input width of $\simeq 100\ \mu m$ at the beam's waist. The formation of a spatial soliton as a function of the input peak power is shown in Fig. 5(a) for a coupling location that is far away from the mirror, *i.e.* in an homogeneous region.

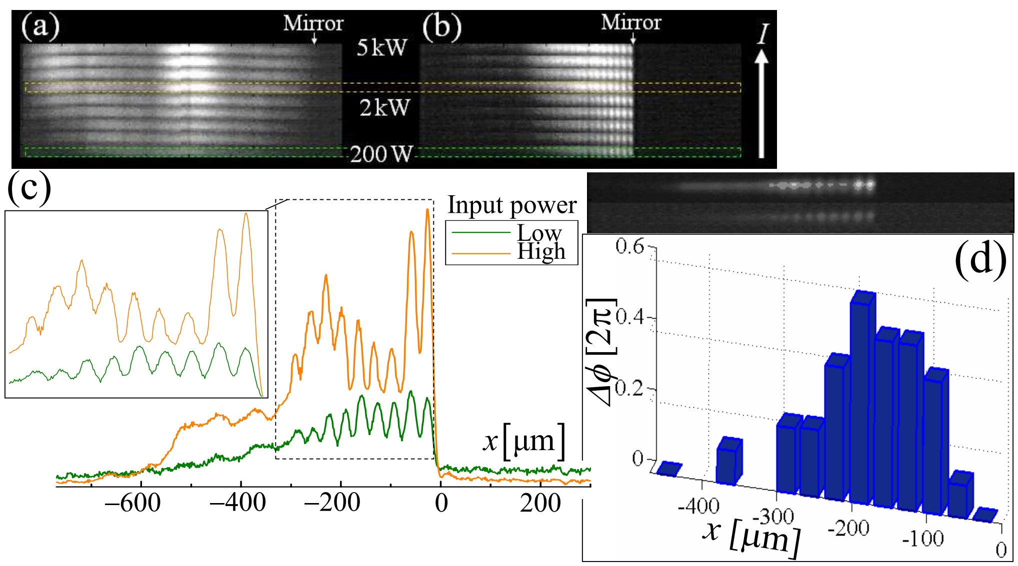

Fig. 5. Experimental results of phase shift profile estimation in the weak perturbation regime: **(a), (b)** Formation of a spatial soliton as a function of input peak power in **(a)** an homogeneous region ($p \simeq 0$ in Fig. 4(d)), and **(b)** in proximity to the mirror ($p \simeq 400\ \mu m$). **(c)** Low power (green) and high power (orange) interference fringe patterns of the output beam. **(d)** The soliton's lateral phase shift profile as extracted from (c).

As the coupling location is in the weak perturbation regime, the spatial soliton that is formed is accompanied by a positive phase shift in the fringe pattern (Fig. 5(b)). Following integration along the vertical axis (Fig. 5(c)), the comparison between the fringe positions in low power (green) and in soliton power (orange) yields the relative phase shifts of the interference patterns.

#84738 - $15.00 USD Received 2 Jul 2007; revised 30 Aug 2007; accepted 2 Sep 2007; published 6 Sep 2007
(C) 2007 OSA

Note that the fringe movement is gradual between adjacent fringes, implying a slowly-varying phase profile. By the arguments discussed in Sections 1 and 2, we can infer that in the first approximation (that is applicable as long as the mirror perturbation is weak) the phase shift is exactly equal to the soliton's local phase increase. The extracted soliton's lateral phase shift profile is shown in Fig. 5(d). This result is in qualitative agreement with the corresponding numerical simulation (Fig. 2(a)).

3.2. Observation of sharp phase gradients

By applying tilts to the input beam relative to the sample, different excitation conditions were explored, *i.e.* with initial conditions in which the input phase front is not flat. An interesting phenomenon that we have observed in such cases was the occurrence of a series of nonlinearity-induced sharp phase shifts (larger than 2π) at x separations that are smaller than the fringe period, even when the excitation is in the weak perturbation regime. An example is shown in Fig. 6(a). Sharp nonlinear phase gradients, which are extended in x, were observed as local "blurring" of the interference pattern around these regions, as shown in Fig. 6(b).

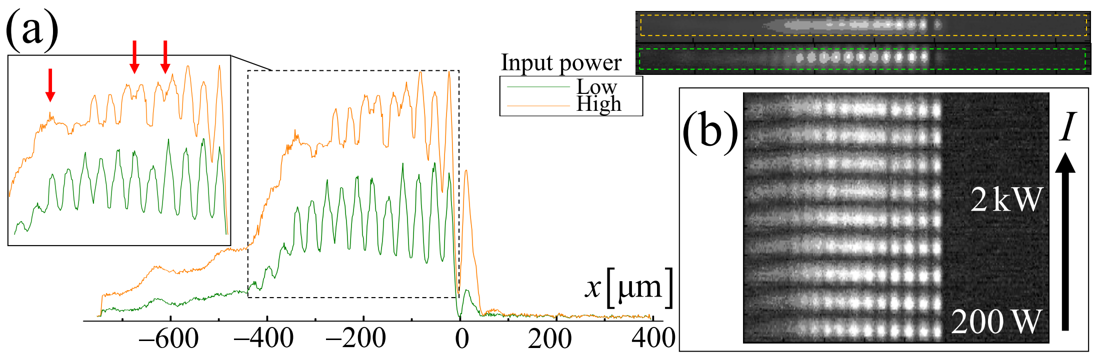

Fig. 6. Experimental results of sharp phase gradients with a non-flat input phase front in the weak perturbation regime: **(a)** Interference fringe patterns exhibiting sharp phase gradients (indicated by the red arrows). **(b)** An example of local phase "blurring" as a function of the power, induced by sharp nonlinear phase gradients.

3.3. Strong perturbation regime

As the beam is coupled in close proximity to the mirror (lower part of Fig. 4(d) with $p > 800$ μm), the power-dependent characteristics of the interference pattern are substantially different.

As shown in Fig. 7(a), in this case there is an increase in the number of visible fringes for a high power input beam, in comparison to a low power excitation. The discrete Fourier transforms of these scans (Fig. 7(b)) confirms that new spatial frequency components k_x appear in the spectrum of the interference pattern in the intermediate and high power cases.

We speculate that these new harmonics are signatures of cross phase modulation and wave mixing [15−18] between the original and reflected components, as both of them now possess comparable high power. We also note that there are a few other possibilities, such as the resonant scattering of dispersive waves by the soliton [19] and nonlinearity-induced ground state selection [20], which can be regarded as a four-wave mixing process [21]. In any event, phase retrieval is impossible using simple imaging in the strong perturbation regime, as the physical influence of the mirror becomes substantial rather than perturbative.

#84738 - $15.00 USD Received 2 Jul 2007; revised 30 Aug 2007; accepted 2 Sep 2007; published 6 Sep 2007
(C) 2007 OSA

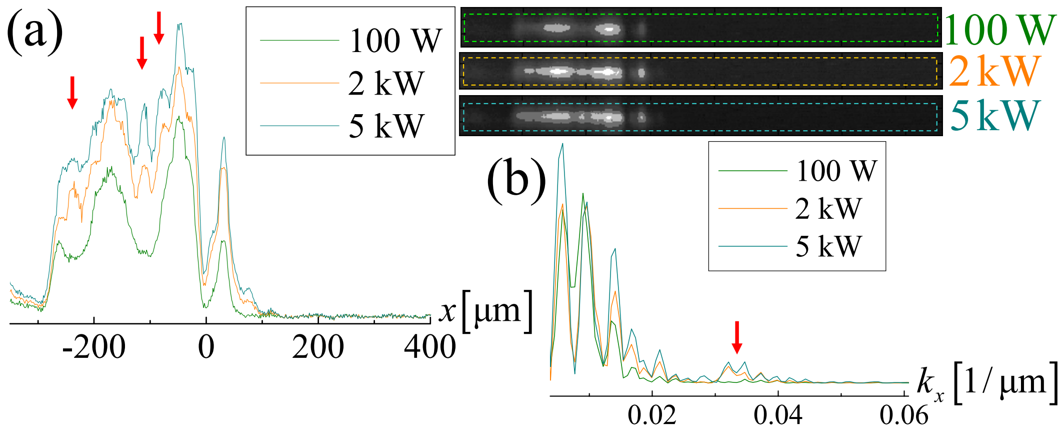

Fig. 7. Experimental results in the strong perturbation regime ($p \simeq 1200\ \mu m$). **(a)** Low power (green), intermediate power (orange) and high power (cyan) interference fringe patterns of the output beam. **(b)** Discrete Fourier transforms of the data in (a) showing the transverse spatial frequency content of the light emerging from the waveguide.

4. Conclusion

We have introduced a unique single beam method for the single shot measurement of phase shift profiles formed in spatial solitons, following their propagation through 2D slab nonlinear waveguides. The method uses a lithographically etched reflective surface positioned near the beam's launching position. In addition to phase shift profile mapping in spatial solitons, this setup enabled us to observe nonlinearity-induced sharp phase gradients, and to record the creation of high spatial harmonics as the beam is launched in near proximity to the mirror surface.

Acknowledgments

We gratefully acknowledge financial support by the Israel Science Foundation (ISF), through grants 8006/03 and 944/05, and by the Natural Sciences and Engineering Research Council of Canada (NSERC). We thank Prof. Victor Fleurov and his student Gali Dekel for fruitful discussions regarding different aspects of this work.